AIMS Mathematics

https://www.aimspress.com/journal/Math

AIMS Mathematics, 11(8): 25861–25873.
DOI: 10.3934/math.20261036
Received: 04 July 2026
Revised: 06 August 2026
Accepted: 18 August 2026
Published: 20 August 2026

Research article

Dynamical analysis of (2+1)-dimensional Akbota-Myrzakulov-Tolkynay-Zhaidary equation: Bifurcations, chaos, and traveling wave solutions

Da Shi and Zhao Li*

College of Computer Science, Chengdu University, Chengdu, 610106, China

* **Correspondence:** Email: lizhao@cdu.edu.cn.

Abstract: This article conducted a systematic dynamical study on the Akbota-Myrzakulov-Tolkynay-Zhaidary (AMTZ) equation, with a focus on its traveling wave solutions, bifurcations, and chaotic phenomena. First, the AMTZ equation was transformed into a nonlinear ordinary differential equation using traveling wave transformation. Based on the polynomial complete discriminant system method, various exact traveling wave solutions of the equation were obtained, including Jacobi elliptic function solutions, implicit solutions, and rational function solutions. Second, using the phase plane analysis method, the corresponding two-dimensional planar dynamical system and its dynamic behavior under small disturbances were studied, revealing the bifurcation characteristics of the equilibrium point. Finally, three-dimensional waveform diagrams, two-dimensional profile diagrams, and contour maps of typical solutions were provided through numerical simulations, visually demonstrating the rich wave propagation modes and spatial structures of the AMTZ equation.

Keywords: Akbota-Myrzakulov-Tolkynay-Zhaidary equation; exact solution; chaotic behavior; phase portrait
Mathematics Subject Classification: 34C23, 35B20, 35C05, 35C07

1. Introduction

In recent years, the study of traveling wave solutions and their dynamic behavior of high-dimensional nonlinear partial differential equations (NLPDEs) have become one of the hotspots [1–3]. Usually, high-dimensional NLPDEs can be transformed into nonlinear ordinary differential equations (NLODEs) using traveling wave transformation [4–6]. If NLODE is a coupled system, it can be assumed that its unknown variables satisfy a linear transformation relationship, thus simplifying the system of equations into a single NLODE, and using the method of constructing traveling wave solutions of NLPDEs to obtain the traveling wave solution of the original system [7, 8].

If the NLPDE system is coupled, but the simplified variables satisfy specific relationships, then the problem of constructing traveling wave solutions for NLPDEs can be transformed into a problem of constructing traveling wave solutions for a single NLPDE [9, 10]. Common construction methods include generalized (G'/G)-expansion method [11], F-expansion method [12], the complete discriminant system method [13], the planar dynamic system analysis method [14–16], the enhanced direct algebraic method [17], the bilinear neural network method [18, 19], the artificial neural network method [20], the modified extended direct algebraic method [21], the asymptotic expansion method [22, 23], and other methods [24–26].

The Akbota-Myrzakulov-Tolkynay-Zhaidary (AMTZ) equation is a very important (2+1)-dimensional NLPDE, which is usually described as follows [27]

$$\begin{cases} q_t - \frac{1}{b}uq_x + \frac{\beta}{b}qq_y - \beta r_y = 0, \\ r_t - \frac{1}{b}ur_x + \frac{\beta}{b}rq_y - \frac{\beta}{4ab}q_{xxy} = 0, \\ u_x + \frac{\beta}{2}q_y = 0, \end{cases} \tag{1.1}$$

where $q = q(t, x, y)$, $r = r(t, x, y)$, and $u = u(t, x, y)$ represent unknow functions. q, R, and u respectively represent the wave function related to spin component, magnetic permeability related quantity, and convective velocity field. The parameters a, b, and β are real constants. The parameter a represents the anisotropy strength of the medium, β is the nonlinear coupling coefficient, and b corresponds to the drift rate of the background flow. In reference [27], Mahmood and Murad studied the soliton solutions, bifurcations, and dynamical behaviors of Eq (1.1).

The remainder of this article is structured in the following manner: In Section 2, the AMTZ equation is transformed into a system of NLODEs by using traveling wave transformation. In Section 3, the complete discriminant system method of polynomials is applied to construct the traveling wave solution of the AMTZ equation. In Section 4, the dynamic behavior of binary dynamical systems and their periodic systems is studied. In Section 5, the three-dimensional (3D) plots, two-dimensional (2D) profiles, density distributions, and polar diagrams of representative solutions of Eq (1.1) are presented under specific parameter settings. In Section 6, a brief conclusion is given.

2. Traveling wave transformation

For the system of Eq (1.1), we make the following traveling wave transformation

$$q(t, x, y) = q(\xi), \;\; r(t, x, y) = r(\xi), \;\; u(t, x, y) = u(\xi), \;\; \xi = kx + ly + vt, \tag{2.1}$$

where k, l, and v are nonzero constants.

Plugging Eq (2.1) into Eq (1.1), we obtain the nonlinear ordinary differential equations

$$\begin{cases} vq' - \frac{k}{b}uq' + \frac{\beta l}{b}qq' - \beta lr' = 0, \\ vr' - \frac{k}{b}ur' + \frac{\beta l}{b}rq' - \frac{\beta k^2 l}{4ab}q''' = 0, \\ ku' + \frac{\beta l}{2}q' = 0. \end{cases} \tag{2.2}$$

Integrating the third equation of Eq (2.2) yields

$$u = -\frac{\beta l}{2k}q + c_1, \tag{2.3}$$

where c_1 is the integration constant.

Substituting Eq (2.3) into the first and second equations of Eq (2.2) yields

$$\begin{cases} vq' - \frac{k}{b}(-\frac{\beta l}{2k}q + c_1)q' + \frac{\beta l}{b}qq' - \beta l r' = 0, \\ vr' - \frac{k}{b}(-\frac{\beta l}{2k}q + c_1)r' + \frac{\beta l}{b}rq' - \frac{\beta k^2 l}{4ab}q''' = 0. \end{cases} \tag{2.4}$$

Integrating the first equation of Eq (2.4) and simplifying it, we can obtain

$$r = c_4q^2 + c_3q + c_2, \tag{2.5}$$

where $c_3 = \frac{1}{\beta l}(v - \frac{k}{b}c_1)$, $c_4 = \frac{3}{4b}$. c_2 is the integration constant.

Taking the derivative of Eq (2.5) and substituting it into the second equation of Eq (2.4), and then integrating it, we can obtain

$$q'' = d_3q^3 + d_2q^2 + d_1q + d_0, \tag{2.6}$$

where $d_3 = \frac{4ac_4}{3k^2 v}(1 + v)$, $d_2 = \frac{ac_3}{k^2 v}(4bc_4\beta v + 1 + 2v)$, $d_1 = \frac{4a}{k^2}(c_3^2 b + c_2)$. d_0 is the integration constant.

3. Exact solutions of Eq (1.1)

Multiplying both sides of Eq (2.6) by q' simultaneously, we can integrate to obtain

$$(\frac{dq}{d\xi})^2 = \frac{d_3}{2}q^4 + \frac{2d_2}{3}q^3 + d_1q^2 + 2d_0q + 2d, \tag{3.1}$$

where d is the integration constant.

When $d_3 > 0$, we make the transformation $\Phi = (\frac{d_3}{4})^{\frac{1}{4}}(q + \frac{d_2}{3d_3})$ and $\xi_1 = (\frac{d_3}{4})^{\frac{1}{4}}\xi$, and substitute this transformation into Eq (3.1) to obtain

$$(\frac{d\Phi}{d\xi_1})^2 = \Phi^4 + \chi_2\Phi^2 + \chi_1\Phi + \chi_0, \tag{3.2}$$

where $\chi_2 = \frac{\sqrt{2}d_1}{\sqrt{d_3}}$, $\chi_1 = (\frac{4d_2^3}{27d_3^2} - \frac{2d_1d_2}{3d_3} + 2d_0)(\frac{d_3}{2})^{-\frac{1}{4}}$ and $\chi_0 = -\frac{d_2^4}{54d_3^4} + \frac{d_1d_2^2}{9d_3^2} - \frac{2d_0d_2}{3d_3} + 2d$.

When $d_3 < 0$, we make the transformation $\Phi = (-\frac{d_3}{4})^{\frac{1}{4}}(q + \frac{d_2}{3d_3})$, and $\xi_1 = (-\frac{d_3}{4})^{\frac{1}{4}}\xi$, and substitute this transformation into Eq (3.1) to obtain

$$(\frac{d\Phi}{d\xi_1})^2 = -(\Phi^4 + \chi_2\Phi^2 + \chi_1\Phi + \chi_0), \tag{3.3}$$

where $\chi_2 = \frac{-\sqrt{2}d_1}{\sqrt{-d_3}}$, $\chi_1 = (-\frac{4d_2^3}{27d_3^2} + \frac{2d_1d_2}{3d_3} - 2d_0)(-\frac{d_3}{2})^{-\frac{1}{4}}$, and $\chi_0 = \frac{d_2^4}{54d_3^4} - \frac{d_1d_2^2}{9d_3^2} + \frac{2d_2}{3d_3} - 2d$.

Thus, Eqs (3.2) and (3.3) can be transformed to

$$\pm(\xi_1 - \xi_0) = \int \frac{d\Phi}{\sqrt{\varepsilon(\Phi^4 + \chi_2\Phi^2 + \chi_1\Phi + \chi_0)}} = \int \frac{d\Phi}{\sqrt{\varepsilon F(\Phi)}}, \tag{3.4}$$

where ξ_0 is an integral constant, $\varepsilon = \pm 1$.

According to the complete discriminant system for fourth order polynomials [28, 29]

$$\begin{cases} D_1 = 4, \\ D_2 = -\chi_2, \\ D_3 = -2\chi_2^3 + 8\chi_2\chi_0 - 9\chi_1^2, \\ D_4 = -\chi_2^3\chi_1^2 + 4\chi_2^4\chi_0 + 36\chi_2\chi_1^2\chi_0 - 32\chi_2^2\chi_0^2 - \frac{27}{4}\chi_1^4 + 64\chi_0^3, \\ E_2 = 9\chi_2^2 - 32\chi_2\chi_0, \end{cases} \tag{3.5}$$

the roots of quartic polynomials are $F(\Phi) = \Phi^4 + \chi_2\Phi^2 + \chi_1\Phi + \chi_0$. By using the Liu's method (see [29]), the solutions of Eq (1.1) are obtained as:

Case 1. When $D_2 < 0$, $D_3 = 0$, $D_4 = 0$, $F(\Phi)$ possesses a pair of conjugate complex roots, specifically: $F(\Phi) = [(\Phi - \vartheta_1)^2 + \vartheta_2^2]^2$, where ϑ_1 and ϑ_2 are both real numbers, and $\vartheta_2 > 0$.

Under these conditions, Eq (3.4) can be transformed into the following form

$$\pm\sqrt[4]{\frac{d_3}{4}}(\xi - \xi_0) = \int \frac{d\Phi}{(\Phi - \vartheta_1)^2 + \vartheta_2^2} = \frac{1}{\vartheta_2}\arctan\frac{\Phi - \vartheta_1}{\vartheta_2}. \tag{3.6}$$

Consequently, the periodic solution of the trigonometric function in of Eq (1.1) is obtained as

$$q_1(t, x, y) = \sqrt[4]{\frac{4}{d_3}}[\vartheta_2\tan(\vartheta_2\sqrt[4]{\frac{d_3}{4}}(kx + ly + vt - \xi_0)) + \vartheta_1] - \frac{d_2}{3d_3}. \tag{3.7}$$

Case 2. When $D_2 = 0$, $D_3 = 0$, $D_4 = 0$, the function $F(\Phi)$ has a single quadruple root, specifically: $F(\Phi) = \Phi^4$.

Substituting $F(\Phi) = \Phi^4$ into Eq (3.4), the rational function solution of Eq (1.1) can be obtained:

$$q_2(t, x, y) = -\sqrt{\frac{4}{d_3}}\frac{1}{kx + ly + vt - \xi_0} - \frac{d_2}{3d_3}. \tag{3.8}$$

Case 3. When $D_2 > 0$, $D_3 = 0$, $D_4 = 0$, $E_2 > 0$, $F(\Phi)$ has two distinct double real roots, i.e., $F(\Phi) = (\Phi - \vartheta_3)^2(\Phi - \vartheta_4)^2$, where ϑ_3 and ϑ_4 are both real numbers, and $\vartheta_3 > \vartheta_4$.

Starting from Eq (3.4), we can derive that when $\varepsilon = 1$, $\Phi > \vartheta_3$, or $\Phi < \vartheta_4$,

$$\pm\sqrt[4]{\frac{d_3}{4}}(\xi - \xi_0) = \int \frac{d\Phi}{(\Phi - \vartheta_3)(\Phi - \vartheta_4)} = \frac{1}{\vartheta_3 - \vartheta_4}\ln|\frac{\Phi - \vartheta_3}{\Phi - \vartheta_4}|. \tag{3.9}$$

When $\Phi > \vartheta_3$ or $\Phi < \vartheta_4$, the solution to Eq (1.1) can be derived:

$$q_3(t, x, y) = \sqrt[4]{\frac{4}{d_3}}[\frac{\vartheta_4 - \vartheta_3}{2}(\coth(\frac{1}{2}\sqrt[4]{\frac{d_3}{4}}(\vartheta_3 - \vartheta_4)(kx + ly + vt - \xi_0)) - 1) + \vartheta_4] - \frac{d_2}{3d_3}. \tag{3.10}$$

When $\vartheta_4 < \Phi < \vartheta_3$, the solution to Eq (1.1) takes the form:

$$q_4(t, x, y) = \sqrt[4]{\frac{4}{d_3}}[\frac{\vartheta_4 - \vartheta_3}{2}(\tanh(\frac{1}{2}\sqrt[4]{\frac{d_3}{4}}(\vartheta_4 - \vartheta_3)(kx + ly + vt - \xi_0)) - 1) + \vartheta_4] - \frac{d_2}{3d_3}. \tag{3.11}$$

Case 4. When $D_2 > 0$, $D_3 > 0$, $D_4 = 0$, $F(\Phi)$ has one double real root and two distinct real roots, i.e., $F(Q) = (\Phi - \mu_1)^2(\Phi - \mu_2)(\Phi - \mu_3)$, where μ_1, μ_2, and μ_3 are real numbers, and $\mu_2 > \mu_3$.

Subcase 4.1. $\varepsilon = 1$

When $\mu_1 > \mu_2$ and $\Phi > \mu_2$, or $\mu_1 < \mu_3$ and $\Phi < \mu_3$, the implicit function solution of Eq (1.1) can be derived from Eq (3.4) as:

$$\pm\sqrt[4]{\frac{d_3}{4}}(\xi - \xi_0) = \frac{1}{(\mu_1 - \mu_2)(\mu_1 - \mu_3)} \ln \frac{[\sqrt{(\Phi - \mu_2)(\mu_1 - \mu_3)} - \sqrt{(\mu_1 - \mu_2)(\Phi - \mu_3)}]^2}{|\Phi - \mu_1|}. \tag{3.12}$$

When $\mu_1 > \mu_2$ and $\Phi < \mu_3$, or $\mu_1 < \mu_3$ and $\Phi < \mu_2$, the implicit function solution of Eq (1.1) can be derived from Eq (3.4) as:

$$\pm\sqrt[4]{\frac{d_3}{4}}(\xi - \xi_0) = \frac{1}{(\mu_1 - \mu_2)(\mu_1 - \mu_3)} \ln \frac{[\sqrt{(\Phi - \mu_2)(\mu_3 - \mu_1)} - \sqrt{(\mu_2 - \mu_1)(\Phi - \mu_3)}]^2}{|\Phi - \mu_1|}. \tag{3.13}$$

When $\mu_2 > \mu_1 > \mu_3$, the implicit function solution of Eq (1.1) can be derived from Eq (3.4) as:

$$\pm\sqrt[4]{\frac{d_3}{4}}(\xi - \xi_0) = \frac{1}{(\mu_2 - \mu_1)(\mu_1 - \mu_3)} \arcsin \frac{(\Phi - \mu_2)(\mu_1 - \mu_3) + (\mu_1 - \mu_2)(\Phi - \mu_3)}{|(\Phi - \mu_1)(\mu_2 - \mu_3)|}. \tag{3.14}$$

Subcase 4.2. $\varepsilon = -1$

When $\mu_1 > \mu_2$ and $\Phi > \mu_2$, or $\mu_1 < \mu_3$ and $\Phi < \mu_3$, the implicit function solution of Eq (1.1) can be derived from Eq (3.4) as:

$$\pm\sqrt[4]{\frac{d_3}{4}}(\xi - \xi_0) = \frac{1}{(\mu_2 - \mu_1)(\mu_1 - \mu_3)} \ln \frac{[\sqrt{(-\Phi + \mu_2)(\mu_1 - \mu_3)} - \sqrt{(\mu_2 - \mu_1)(\Phi - \mu_3)}]^2}{|\Phi - \mu_1|}. \tag{3.15}$$

When $\mu_1 > \mu_2$ and $\Phi < \mu_3$, or $\mu_1 < \mu_3$ and $\Phi < \mu_2$, the implicit function solution of Eq (1.1) can be derived from Eq (3.4) as:

$$\pm\sqrt[4]{\frac{d_3}{4}}(\xi - \xi_0) = \frac{1}{(\mu_2 - \mu_1)(\mu_1 - \mu_3)} \ln \frac{[\sqrt{(-\Phi + \mu_2)(\mu_3 - \mu_1)} - \sqrt{(\mu_1 - \mu_{21})(\Phi - \mu_3)}]^2}{|\Phi - \mu_1|}. \tag{3.16}$$

When $\mu_2 > \mu_1 > \mu_3$, the implicit function solution of Eq (1.1) can be derived from Eq (3.4) as:

$$\pm\sqrt[4]{\frac{d_3}{4}}(\xi - \xi_0) = \frac{1}{(\mu_1 - \mu_2)(\mu_1 - \mu_3)} \arcsin \frac{(-\Phi + \mu_2)(\mu_1 - \mu_3) + (\mu_2 - \mu_1)(\Phi - \mu_3)}{|(\Phi - \mu_1)(\mu_2 - \mu_3)|}. \tag{3.17}$$

Case 5. When $D_2 > 0$, $D_3 = 0$, $D_4 = 0$, $E_2 = 0$, $F(\Phi) = (\Phi - \mu_4)^3(\Phi - \mu_5)$, where μ_4 and μ_5 are both real numbers.

Subcase 5.1. $\varepsilon = 1$

When $\Phi > \mu_4$ and $\Phi > \mu_5$, or $\Phi < \mu_4$ and $\Phi < \mu_5$, the solution to Eq (1.1) takes the form:

$$q_5(t, x, y) = \sqrt[4]{\frac{4}{d_3}}\left(\frac{4(\mu_4 - \mu_5)}{(\mu_5 - \mu_4)^2 \sqrt{\frac{d_3}{4}}(kx + ly + vt - \xi_0)^2 - 4} + \mu_4\right) - \frac{d_2}{3d_3}. \tag{3.18}$$

Subcase 5.2. $\varepsilon = -1$

When $\Phi > \mu_4$ and $\Phi < \mu_5$, or $\Phi < \mu_4$ and $\Phi > \mu_5$, the solution to Eq (1.1) takes the form:

$$q_6(t,x,y) = \sqrt[4]{-\frac{4}{d_3}}\left(\frac{4(\mu_4-\mu_5)}{-(\mu_5-\mu_4)^2\sqrt{-\frac{d_3}{4}}(kx+ly+vt-\xi_0)^2-4}+\mu_4\right)-\frac{d_2}{3d_3}. \tag{3.19}$$

Case 6. When $D_2D_3 < 0, D_4 = 0$, $F(\Phi) = (\Phi-\lambda_1)^2[(\Phi-\lambda_2)^2+\lambda_3^2]$, where λ_1, λ_2, and λ_3 are real numbers.

Thus, the solution to Eq (1.1) takes the form:

$$q_7(t,x,y) = \sqrt[4]{\frac{4}{d_3}}\frac{e^{\pm\sqrt{(\lambda_1-\lambda_2)^2+\lambda_3^2}\sqrt[4]{\frac{d_3}{4}}(kx+ly+vt-\xi_0)}-\kappa_1+\sqrt{(\lambda_1-\lambda_2)^2+\lambda_3^2}(2-\kappa_1)}{(e^{\pm\sqrt{(\lambda_1-\lambda_2)^2+\lambda_3^2}\sqrt[4]{\frac{d_3}{4}}(kx+ly+vt-\xi_0)}-\kappa_1)^2-1}-\frac{d_2}{3d_3}, \tag{3.20}$$

where $\kappa_1 = \frac{\lambda_1-2\lambda_2}{\sqrt{(\lambda_1-\lambda_2)^2+\lambda_3^2}}$.

Case 7. When $D_1 > 0$, $D_3 > 0$, $D_4 > 0$, $F(Q)$ has four real roots, i.e., $F(\Phi) = (\Phi-\theta_1)(\Phi-\theta_2)(\Phi-\theta_3)(\Phi-\theta_4)$, where θ_1, θ_2, θ_3, and θ_4 are real numbers, and $\theta_1 > \theta_2 > \theta_3 > \theta_4$.

Subcase 7.1. $\varepsilon = 1$

When $\Phi > \theta_1$ or $\Phi < \theta_4$, the Jacobian sine solutions of Eq (1.1) are

$$q_8(t,x,y) = \sqrt[4]{\frac{4}{d_3}}\frac{\theta_2(\theta_1-\theta_4)\mathbf{sn}^2(\frac{\sqrt{(\theta_1-\theta_3)(\theta_2-\theta_4)}}{2}(\sqrt[4]{\frac{d_3}{4}}(kx+ly+vt-\xi_0),m)-\theta_1(\theta_2-\theta_4)}{(\theta_1-\theta_4)\mathbf{sn}^2(\frac{\sqrt{(\theta_1-\theta_3)(\theta_2-\theta_4)}}{2}\sqrt[4]{\frac{d_3}{4}}(kx+ly+vt-\xi_0),m)-\theta_2+\theta_4}-\frac{d_2}{3d_3}, \tag{3.21}$$

$$q_9(t,x,y) = \sqrt[4]{\frac{4}{d_3}}\frac{\theta_4(\theta_2-\theta_3)\mathbf{sn}^2(\frac{\sqrt{(\theta_1-\theta_3)(\theta_2-\theta_4)}}{2}(\sqrt[4]{\frac{d_3}{4}}(kx+ly+vt-\xi_0),m)-\theta_3(\theta_2-\theta_4)}{(\theta_2-\theta_3)\mathbf{sn}^2(\frac{\sqrt{(\theta_1-\theta_3)(\theta_2-\theta_4)}}{2}\sqrt[4]{\frac{d_3}{4}}(kx+ly+vt-\xi_0),m)-\theta_2+\theta_4}-\frac{d_2}{3d_3}, \tag{3.22}$$

where $m^2 = \frac{(\theta_1-\theta_4)(\theta_2-\theta_3)}{(\theta_1-\theta_3)(\theta_2-\theta_4)}$.

Subcase 7.2. $\varepsilon = -1$

When $\theta_1 > \Phi > \theta_2$, or $\theta_3 > \Phi > \theta_4$, the Jacobian sine solutions of Eq (1.1) are

$$q_{10}(t,x,y) = \sqrt[4]{-\frac{4}{d_3}}\frac{\theta_3(\theta_1-\theta_2)\mathbf{sn}^2(\frac{\sqrt{(\theta_1-\theta_3)(\theta_2-\theta_4)}}{2}(\sqrt[4]{-\frac{d_3}{4}}(kx+ly+vt-\xi_0),n)-\theta_2(\theta_1-\theta_3)}{(\theta_1-\theta_2)\mathbf{sn}^2(\frac{\sqrt{(\theta_1-\theta_3)(\theta_2-\theta_4)}}{2}\sqrt[4]{-\frac{d_3}{4}}(kx+ly+vt-\xi_0),n)-\theta_1+\theta_3}-\frac{d_2}{3d_3}, \tag{3.23}$$

$$q_{11}(t,x,y) = \sqrt[4]{-\frac{4}{d_3}}\frac{\theta_1(\theta_3-\theta_4)\mathbf{sn}^2(\frac{\sqrt{(\theta_1-\theta_3)(\theta_2-\theta_4)}}{2}(\sqrt[4]{-\frac{d_3}{4}}(kx+ly+vt-\xi_0),n)-\theta_4(\theta_3-\theta_1)}{(\theta_3-\theta_4)\mathbf{sn}^2(\frac{\sqrt{(\theta_1-\theta_3)(\theta_2-\theta_4)}}{2}\sqrt[4]{-\frac{d_3}{4}}(kx+ly+vt-\xi_0),n)-\theta_3+\theta_1}-\frac{d_2}{3d_3}, \tag{3.24}$$

where $n^2 = \frac{(\theta_1-\theta_2)(\theta_3-\theta_4)}{(\theta_1-\theta_3)(\theta_2-\theta_4)}$.

Case 8. When $D_2D_3 \geq 0$, $D_4 < 0$, $F(\Phi) = (\Phi-\varkappa_1)(\Phi-\varkappa_2)[(\Phi-\varkappa_3)^2+\varkappa_4^2]$, where $\varkappa_1$, $\varkappa_2$, $\varkappa_3$, and $\varkappa_4$ are both real numbers, $\varkappa_1 > \varkappa_2$, and $\varkappa_3, \varkappa_4 > 0$.

So the Jacobi cosine functions of Eq (1.1) can be depicted as

$$q_{12}(t,x,y)=\sqrt[4]{-\frac{4}{d_3}}\frac{s_1\mathbf{cn}(\frac{\sqrt{2\varkappa_4 e(\varkappa_1-\varkappa_2)}}{2em_1}\sqrt[4]{-\frac{d_3}{4}}(kx+ly+vt-\xi_0),m_1)+s_2}{s_3\mathbf{cn}(\frac{\sqrt{\varkappa_4 e(\varkappa_1-\varkappa_4)}}{2em_1}\sqrt[4]{-\frac{d_3}{4}}(kx+ly+vt-\xi_0),m_1)+s_4}-\frac{d_2}{3d_3}, \tag{3.25}$$

$$q_{13}(t,x,y)=\sqrt[4]{\frac{4}{d_3}}\frac{s_1\mathbf{cn}(\frac{\sqrt{-2\varkappa_4 e(\varkappa_1-\varkappa_2)}}{2em_1}\sqrt[4]{\frac{d_3}{4}}(kx+ly+vt-\xi_0),m_1)+s_2}{s_3\mathbf{cn}(\frac{\sqrt{-\varkappa_4 e(\varkappa_1-\varkappa_4)}}{2em_1}\sqrt[4]{\frac{d_3}{4}}(kx+ly+vt-\xi_0),m_1)+s_4}-\frac{d_2}{3d_3}, \tag{3.26}$$

where $s_1=\frac{1}{2}(\varkappa_4+\varkappa_3)c_3-\frac{1}{2}(\varkappa_1-\varkappa_2)c_4$, $s_2=\frac{1}{2}(\varkappa_1+\varkappa_2)c_4-\frac{1}{2}(\varkappa_1-\varkappa_2)c_3$, $s_3=\varkappa_4-\varkappa_{31}-\frac{\varkappa_4}{e}$, $s_4=\varkappa_1-\varkappa_3-\varkappa_4 e$, $E=\frac{\varkappa_4^2+(\varkappa_1-\varkappa_3)(\varkappa_2-\varkappa_3)}{\varkappa_4(\varkappa_1-\varkappa_2)}$, $e=E-\sqrt{E^2+1}$, and $m_1^2=\frac{1}{1+e^2}$.

Case 9. While $D_2D_3\le 0$, $D_4>0$, $F(\Phi)=[(\Phi-\rho_1)^2+\rho_2^2][(\Phi-\rho_3)^2+\rho_4^2]$, where ρ_1,ρ_2,ρ_3, and ρ_4 are real numbers, and $\rho_3\ge\rho_4>0$.

Then we can obtain the solution of Eq (1.1) as

$$q_{14}(t,x,y)=\sqrt[4]{\frac{4}{d_3}}\frac{\varsigma_1\mathbf{sn}(\eta\sqrt[4]{\frac{d_3}{4}}(kx+ly+vt-\xi_0),r)+\varsigma_2\mathbf{cn}(\eta\sqrt[4]{\frac{d_3}{4}}(kx+ly+vt-\xi_0),r)}{\varsigma_3\mathbf{sn}(\eta\sqrt[4]{\frac{d_3}{4}}(kx+ly+vt-\xi_0),r)+\varsigma_4\mathbf{cn}(\eta\sqrt[4]{\frac{d_3}{4}}(kx+ly+vt-\xi_0),r)}-\frac{d_2}{3d_3}, \tag{3.27}$$

where $\varsigma_1=\rho_1c_3+\rho_3c_4$, $\varsigma_2=\rho_1c_4-\rho_2c_3$, $\varsigma_3=-\rho_3-\frac{\rho_4}{e}$, $\varsigma_4=\rho_1-\rho_3$, $e=E+\sqrt{E^2-1}$, $r^2=\frac{e^2-1}{e^2}$, $E=\frac{(\rho_1-\rho_3)^2+\rho_2^2+\rho_4^2}{2\rho_2\rho_4}$, and $\eta=\frac{\rho_4\sqrt{(\varsigma_3^2+\varsigma_4^2)(\varsigma_3^2e^2+\varsigma_4^2)}}{\varsigma_3^2+\varsigma_4^2}$.

Remark 3.1. *In this section, we reduced the original system of Eq (1.1) to a system of ordinary differential equations using the traveling wave transformation $\xi=kx+ly+vt$, and systematically obtained its rich and accurate traveling wave solutions $q_1(t,x,y),q_2(t,x,y),\cdots,q_{14}(t,x,y)$. These solutions $q(t,x,y)$ are given in the form of explicit functions, covering various types such as solitary wave solutions, periodic wave solutions, twisted and anti-twisted solutions, singular wave solutions, etc. To obtain explicit solutions for the physical variables $u(t,x,y)$ and $r(t,x,y)$ in the original system of Eq (1.1), we need to perform solution reduction. Specifically, each obtained traveling wave solution $q(t,x,y)$ is sequentially substituted into the variable relationship Eqs (2.3) and (2.5), and necessary integration and algebraic operations are performed to obtain the solutions $u(t,x,y)$ and $r(t,x,y)$ expressed explicitly.*

4. Qualitative analysis

Mahmood et al. [27] studied the dynamic behavior of Eq (1.1) via the planar dynamical system method when $d_0=0$. Assuming $\frac{dq}{d\xi}=z$, two-dimensional dynamical system of Eq (2.6) can be written as

$$\begin{cases}\frac{dq}{d\xi}=z,\\ \frac{dz}{d\xi}=d_3q^3+d_2q^2+d_1q+d_0,\end{cases} \tag{4.1}$$

with the Hamiltonian system

$$H(q,z)=\frac{1}{2}z^2-\frac{d_3}{4}q^4-\frac{d_2}{3}q^3-\frac{d_1}{2}q^2-d_0q=h, \tag{4.2}$$

where h is an integration constant.

Adding small periodic disturbances to system (1.1) yields

$$\begin{cases} q_t - \frac{1}{b}uq_x + \frac{\beta}{b}qq_y - \beta r_y = 0, \\ r_t - \frac{1}{b}ur_x + \frac{\beta}{b}rq_y - \frac{\beta}{4ab}q_{xxy} = G(q), \\ u_x + \frac{\beta}{2}q_y = 0, \end{cases} \tag{4.3}$$

where $G(q)$ is a function with small perturbation.

According to the transformation in the second section, we can obtain the following perturbation system

$$\begin{cases} \frac{dq}{d\xi} = z, \\ \frac{dz}{d\xi} = d_3q^3 + d_2q^2 + d_1q + d_0 + f(\xi), \end{cases} \tag{4.4}$$

where $G(\xi) = -\frac{\beta k^2 l}{4ab}f$. $f(\xi) = A_1\cos(k_1\xi) + A_2\sin(k_2\xi)$. A_i and k_i $(i = 1, 2)$ are the constants.

Remark 4.1. *The phase portrait for the system (4.1) with $d_0 = 0$ has been drawn in Figure 1. This article considers the phase portrait of $d_0 \neq 0$.*

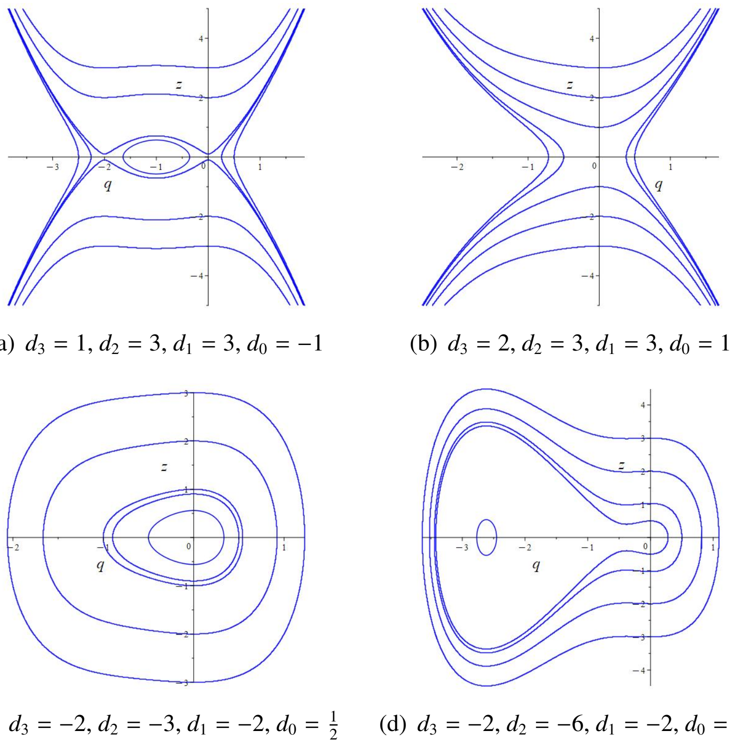

(a) $d_3 = 1, d_2 = 3, d_1 = 3, d_0 = -1$ (b) $d_3 = 2, d_2 = 3, d_1 = 3, d_0 = 1$

(c) $d_3 = -2, d_2 = -3, d_1 = -2, d_0 = \frac{1}{2}$ (d) $d_3 = -2, d_2 = -6, d_1 = -2, d_0 = -2$

Figure 1. Phase portraits of Eq (4.1).

Remark 4.2. *The phase diagram in Figure 2 reveals the global dynamics of the system: Figure 2 (a) presents a complex multi ring entangled structure, exhibiting quasi periodic or weak chaotic states; Figure 2 (b) shows a clear annular limit cycle, corresponding to stable periodic oscillations. The maximum Lyapunov exponent is shown in Figure 3. Figure 4 shows the time series diagram providing* *a time-domain perspective: The $q(\xi)$ corresponding to the Figure 4 (a) exhibits irregular but rhythmic amplitude modulation oscillations, confirming the complexity of the phase diagram; Figure 4 shows a perfect periodic waveform, which corresponds perfectly to the limit cycle in Figure 4 (b).*

(a) $d_3 = -2, d_2 = -3, d_1 = -2, d_0 = \frac{1}{2}$ (b) $d_3 = -2, d_2 = -6, d_1 = -2, d_0 = -2$

Figure 2. Phase portraits of Eq (4.4) with $A_1 = 0.8, A_2 = 0.6, k_1 = 0.8, k_2 = 0.6$.

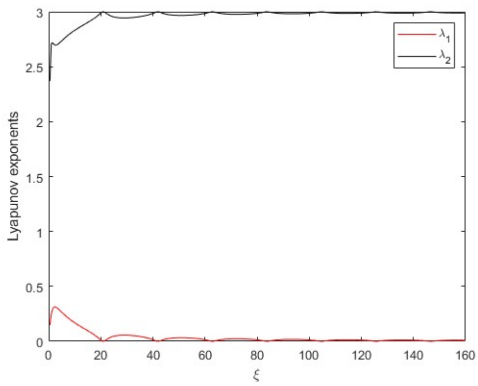

Figure 3. Lyapunov exponents of Eq (4.4) for $d_3 = 1, d_2 = 0.5, d_1 = -2, d_0 = 0.8, A_2 = 0.15, k_2 = 1, A_1 = 0$.

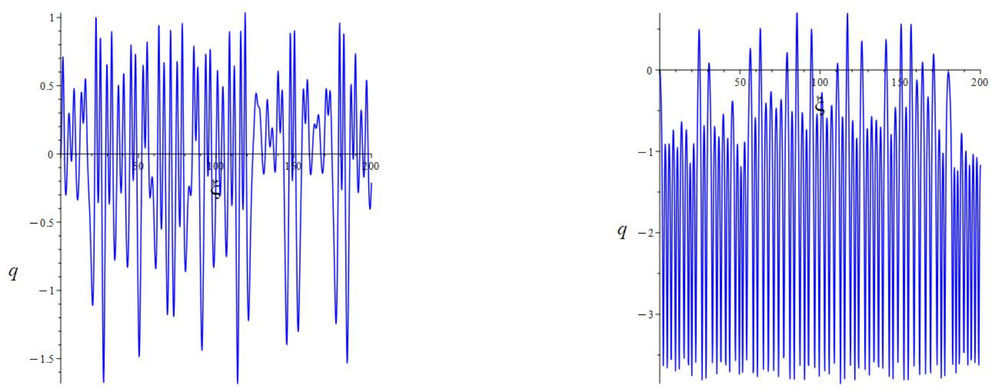

(a) $d_3 = -2, d_2 = -3, d_1 = -2, d_0 = \frac{1}{2}$ (b) $d_3 = -2, d_2 = -6, d_1 = -2, d_0 = -2$

Figure 4. Sensitivity analysis of Eq (4.4) with $A_1 = 0.8, A_2 = 0.6, k_1 = 0.8, k_2 = 0.6$.

5. Numerical simulation

In this section, we have plotted the 3D, 2D, and contour maps of the solutions obtained in the fourth section. Obviously, when $d_3 = 2, d_2 = 3, d_1 = 2, d_0 = \frac{1}{2}, d = \frac{9}{32}, k = 2, l = 1, v = 2$, and $y = 3$, Figure 5 shows a tangent function solution, which is a periodic function solution. When $d_3 = 2, d_2 = 3, d_1 = -5, d_0 = -\frac{7}{4}, d = \frac{59}{32}, k = 2, l = 1, v = 3$, and $y = 3$, Figure 6 shows a Jacobian sine function solution, which is also a periodic function solution.

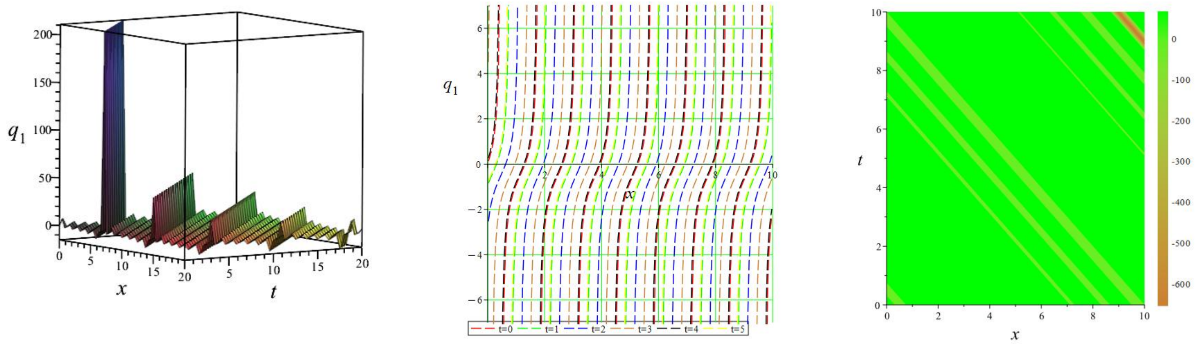

(a) 3D diagram (b) 2D diagram (c) Density plot

Figure 5. Explicit solution $q_1(t, x, y)$ of Eq (1.1) with $d_3 = 2, d_2 = 3, d_1 = 2, d_0 = \frac{1}{2}, d = \frac{9}{32}, k = 2, l = 1, v = 2, y = 3$.

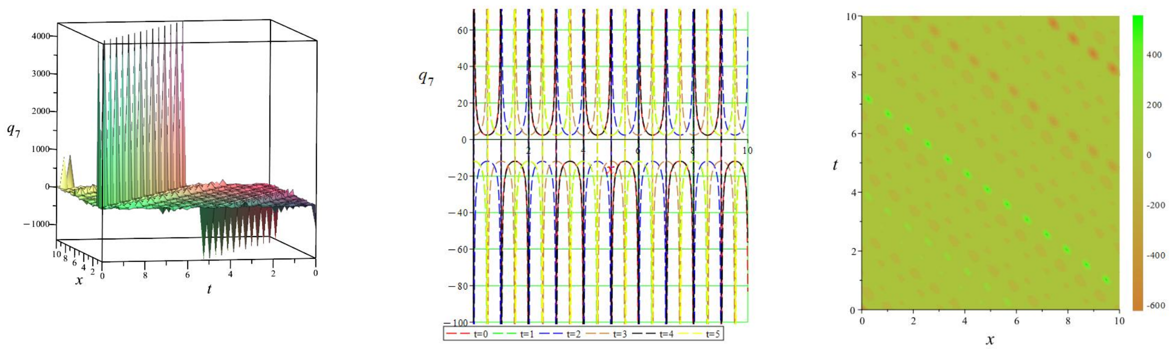

(a) 3D diagram (b) 2D diagram (c) Density plot

Figure 6. Explicit solution $q_7(t, x, y)$ of Eq (1.1) with $d_3 = 2, d_2 = 3, d_1 = -5, d_0 = -\frac{7}{4}, d = \frac{59}{32}, k = 2, l = 1, v = 3, y = 3$.

6. Conclusions

In this study, we conducted a comprehensive dynamic analysis of AMTZ, focusing on its traveling wave solution, bifurcation structure, and chaotic behavior. By using traveling wave transformation, we simplify the AMTZ equation into a nonlinear ordinary differential equation, which is then solved using the polynomial complete discriminant system method. This method enables us to derive a range of rich exact solutions, including Jacobian elliptic function solutions, implicit solutions, and rational function solutions. Through phase plane analysis, we studied the corresponding two-dimensional planar dynamical system, revealed the bifurcation characteristics of the equilibrium point under small disturbances, and demonstrated the transition from a stable periodic orbit to a chaotic attractor with changes in parameters. Numerical simulations further illustrate the complex wave propagation patterns and spatial structures of the AMTZ equation through three-dimensional waveform diagrams, two-dimensional profile diagrams, and contour maps, providing a visual representation of the nonlinear dynamics of the system. Future research may extend this analysis to higher dimensional situations, including external forcing or damping terms, or explore the stability and control of chaotic systems, thereby deepening our understanding of integrable and non integrable nonlinear wave equations.

Author contributions

Z. Li: software, supervision, methodology; D. Shi: writing original draft, writing-review & editing. All authors have read and approved the final version of the manuscript for publication.

Use of Generative-AI tools declaration

The authors declare they have not used artificial intelligence (AI) tools in the creation of this article.

Conflict of interest

All authors declare no conflicts of interest in this paper.

References

1. M. D. Hossain, M. N. Sherif, J. R. M. Borhan, K. El-Rashidy, M. M. Miah, W. X. Ma, Revealing abundant novel optical wave solutions of the two nonlinear models with dynamical behaviors: Bifurcation, chaotic, and stability analyses, *Mod. Phys. Lett. A*, **40** (2025), 2550075. https://doi.org/10.1142/S0217732325500750
2. I. S. Hamad, K. K. Ali, Chaotic phenomena, quasi-periodic, and optical solutions to the third-order (1+1)-nonlinear Schrödinger equation with a power law of self-phase modulation equation, *Ain Shams Eng. J.*, **16** (2025), 103606. https://doi.org/10.1016/j.asej.2025.103606
3. U. Younas, F. Yao, J. Muhammad, Neural network-driven exploration of wave phenomena in ocean and fluid environments, *Ocean Eng.*, **359** (2026), 126056. https://doi.org/10.1016/j.oceaneng.2026.126056
4. S. Guo, L. Mei, Y. Zhou, The compound $(\frac{G'}{G})$-expansion method and double non-traveling wave solutions of (2+1) -dimensional nonlinear partial differential equations, *Comput. Math. Appl.*, **69** (2015), 804–816. https://doi.org/10.1016/j.camwa.2015.02.016

5. K. Zhang, J. Han. Bifurcations of traveling wave solutions for the (2+1)-dimensional generalized asymmetric Nizhnik–Novikov–Veselov equation, *Appl. Math. Comput.*, **251** (2015), 108–117. https://doi.org/10.1016/j.amc.2014.11.041

6. R. Myrzakulov, G. Mamyrbekova, G. Nugmanova, M. Lakshmanan. Integrable (2+1)-dimensional spin models with self-consistent potentials, *Symmetry*, **7** (2015), 1352–1375. https://doi.org/10.3390/sym7031352

7. T. Mathanaranjan, R. Myrzakulov, Integrable Akbota equation: Conservation laws, optical soliton solutions and stability analysis, *Opt. Quant. Electron.*, **56** (2024), 564. https://doi.org/10.1007/s11082-023-06227-0

8. W. B. Rabie, W. Abbas, M. Elsaid Ramadan, H. M. Ahmed, Modulation instability analysis and deriving soliton solutions of new nonlocal Lakshmanan–Porserzian–Daniel equation, *Sci. Rep.*, **15** (2025), 39219. https://doi.org/10.1038/s41598-025-21579-1

9. Z. Li, M. Wu, E. Hussain, Y. Yildirim, Exactly explicit solutions of (2+1)-dimensional conformable fractional diffusive Predator–Prey model via neural networks method, *Front. Phys.*, **14** (2026), 1824530. https://doi.org/10.3389/fphy.2026.1824530

10. Z. Li. Solving the exactly explicit solutions of the conformable space-time fractional Phi-4 equation via neural networks method, *Phys. Lett. A*, **581** (2026), 131535. https://doi.org/10.1016/j.physleta.2026.131535

11. R. Ali, E. Tag-eldin. A comparative analysis of generalized and extended $(\frac{G'}{G})$-expansion methods for travelling wave solutions of fractional Maccari's system with complex structure, *Alex. Eng. J.*, **79** (2023), 508–530. https://doi.org/10.1016/j.aej.2023.08.007

12. M. Borg, N. M. Badra, H. M. Ahmed, W. B. Rable, Solitons behavior of Sasa-Satsuma equation in birefringent fibers with Kerr law nonlinearity using extended F-expansion method, *Ain Shams Eng. J.*, **15** (2024), 102290. https://doi.org/10.1016/j.asej.2023.102290

13. D. Shi, Z. Li. New soliton solutions of the conformable time fractional Drinfel'd–Sokolov–Wilson equation based on the complete discriminant system method, *Open Phys.*, **22** (2024), 20240099. https://doi.org/10.1515/phys-2024-0099

14. Z. Li, E. Hussain, Bifurcation analysis and chaotic behaviors of and a traveling-wave solution to the Zhiber–Shabat Equation with a truncated M-Fractional derivative, *Fractal Fract.*, **10** (2026), 335. https://doi.org/10.3390/fractalfract10050335

15. Z. Manzoor, F. Ashraf, M. Inc, B. Ceesay. Stochastic soliton solutions of ion sound and Langmuir wave equation via new extended direct algebraic method with bifurcation and modulation instability analyses, *AIP Adv.*, **15** (2025), 125212. https://doi.org/10.1063/5.0299876

16. K. Zhang, Z. Ge, J. Cao. Novel insights into the truncated M-fractional Shynaray-IIA equation: New wave solutions and its dynamic behavior, *Netw. Heterog. Media*, **21** (2026), 1197–1226. https://doi.org/10.3934/nhm.2026048

17. H. Lv. Exact traveling wave solutions of the Paraxial wave equation with conformable fractional derivative using an enhanced direct algebraic method, *Symmetry*, **18** (2026), 1300. https://doi.org/10.3390/sym18081300

18. S. Singh, A. Panda, S. S. Ray. Exploring soliton, breather and lump structures in the (4+1)-dimensional KdV-CBS equation with the bilinear neural network method, *Mod. Phys. Lett. B*, **40** (2026), 2650039. https://doi.org/10.1142/S0217984926500399
19. D. Shi, Z. Li. Neural network-driven exact solutions for the conformal nonlinear fractional Kolmogorov-Petrovskii-Piskunov model, *Phys. Lett. A*, **593** (2026), 132023. https://doi.org/10.1016/j.physleta.2026.132023
20. W. Razzaq, A. Zafar, A. A. Nuaim, A. A. Nuaim. A WAS neural network framework for computing and analyzing solutions of a generalized (3+1)-dimensional nonlinear Wave equation: Stability analysis, *AIMS Mathematics*, **11** (2026), 10694–10715. https://doi.org/10.3934/math.2026440
21. M. Arshad, A. R. Seadawy, D. Lu, J. Wang, Travelling wave solutions of Drinfel'd-Sokolov-Wilson, Whitham–Broer–Kaup and (2+1)-dimensional Broer–Kaup–Kupershmit equations and their applications, *Chinese J. Phys.*, **55** (2017), 780–797. https://doi.org/10.1016/j.cjph.2017.02.008
22. M. V. Flamarion, E. Pelinovsky. Interaction of interfacial waves with an external force: the Benjamin-Ono Equation framework *Symmetry*, **15** (2023), 14789. https://doi.org/10.3390/sym15081478
23. M. V. Flamarion, E. Pelinovsky. Interactions of solitons with an external force field: Exploring the Schamel equation framework *Chaos Soliton. Fract.*, **174** (2023), 113799. https://doi.org/10.1016/j.chaos.2023.113799
24. J. Yu, Y. Sun. Exact traveling wave solutions to the (2+1)-dimensional Biswas-Milovic equations, *Optik*, **149** (2017), 378–383. https://doi.org/10.1016/j.ijleo.2017.09.023
25. M. V. Flamarion, E. Pelinovsky, E. Didenkulova. Soliton dynamics in random fields: The Benjamin-Ono equation framework, *Appl. Math. Model.*, **144** (2025), 116092. https://doi.org/10.1016/j.apm.2025.116092
26. K. J. Wang, K. H. Yan, S. Li. Multi-rogue wave, generalized breathers wave, bell shape and singular wave solutions to the (3+1)-dimensional Yu-Toda-Sasa-Fukuyama equation *Math. Method. Appl. Sci.*, **49** (2026), 12139–12152. https://doi.org/10.1002/mma.70663
27. S. S. Mahmood, M. A. S. Murad. Investigation of the soliton solutions, bifurcation analysis, and chaotic nature of the Akbota-Myrzakulov-Tolkynay-Zhaidary equation, *Commun. Theor. Phys.*, **78** (2026), 085002. https://doi.org/10.1088/1572-9494/ae6a79
28. C. S. Liu. Applications of complete discrimination system for polynomial for classifications of traveling wave solutions to nonlinear differential equations, *Comput. Phys. Commun.*, **181** (2010), 317–324. https://doi.org/10.1016/j.cpc.2009.10.006
29. C. S. Liu. Exact travelling wave solutions for (1+1)-dimensional dispersive long wave equation, *Chinese Phys.*, **14** (2005), 1710–1715. https://doi.org/10.1088/1009-1963/14/9/005